Citation: Kandala SS, Uchida TK, Vyasarayani CP. Pole placement for delay differential equations with time-periodic delays using Galerkin approximations. Journal of Computational and Nonlinear Dynamics 16(9): 091007, 2021. doi: 10.1115/1.4051590.

Pole placement for delay differential equations with time-periodic delays using Galerkin approximations

(CND-20-1378, Accepted Manuscript)

Shanti Swaroop Kandala[a], Thomas K. Uchida[b,*], C. P. Vyasarayani[a]

[a] Department of Mechanical and Aerospace Engineering, Indian Institute of Technology Hyderabad
Kandi, Sangareddy, Telangana 502285, India

[b] Department of Mechanical Engineering, University of Ottawa
161 Louis-Pasteur, Ottawa, Ontario, K1N 6N5, Canada

[*] Address all correspondence to this author. E-mail address: tuchida@uottawa.ca

June 18, 2021

Abstract

Many practical systems have inherent time delays that cannot be ignored; thus, their dynamics are described using delay differential equations (DDEs). The Galerkin approximation method is one strategy for studying the stability of time-delay systems. In this work, we consider delays that are time-varying and, specifically, time-periodic. The Galerkin method can be used to obtain a system of ordinary differential equations (ODEs) from a second-order time-periodic DDE in two ways: either by converting the DDE into a second-order time-periodic partial differential equation (PDE) and then into a system of second-order ODEs, or by first expressing the original

DDE as two first-order time-periodic DDEs, then converting into a system of first-order time-periodic PDEs, and finally converting into a first-order time-periodic ODE system. The difference between these two formulations in the context of control is presented in this paper. Specifically, we show that the former produces spurious Floquet multipliers at a spectral radius of 1. We also propose an optimization-based framework to obtain feedback gains that stabilize closed-loop control systems with time-periodic delays. The proposed optimization-based framework employs the Galerkin method and Floquet theory, and is shown to be capable of stabilizing systems considered in the literature. Finally, we present experimental validation of our theoretical results using a rotary inverted pendulum apparatus with inherent sensing delays as well as additional time-periodic state-feedback delays that are introduced deliberately.

Keywords: control system; delay differential equation; Floquet theory; Galerkin approximation; stability; time-delay system.

1 Introduction

In the last decade, the study of time-delay systems (TDS) has found increased application across many domains, including control systems, machining processes, lasers, biological systems, neural networks, and fluid mechanics. In the absence of delays, or if the delays are ignorable, the dynamics of many of these systems can be described simply using ordinary differential equations (ODEs). When delays are present, however, the dynamics are described using delay differential equations (DDEs), where the state derivatives are explicit functions of past states. This property complicates the stability analysis of TDS. In general, delays can be either constant or time-varying. In this work, we consider a special class of time-varying delays in which the delays are time-periodic.

The stability of a TDS depends on the location of the rightmost characteristic root of the system. The stability characteristics of TDS with *constant* delays have been studied extensively in the literature [1, 2]. To determine the stability of a DDE with constant delays, knowledge of its characteristic roots is essential. Several methods have been proposed to determine the characteristic roots of DDEs with constant delays, such as the Lambert W function [1, 3–5], Galerkin approximations [2, 6, 7], Laplace transforms [8], semi-discretization [9], spectral Tau methods [10], and pseudo-spectral collocation [11–13]. A review of the various methods to find the characteristic roots of DDEs with constant delays can be found in Pekař and Gao [14].

The stability analysis of TDS with *time-periodic* delays is not as straightforward as when the delays are constant. The dynamics of a TDS with time-periodic delays (or time-periodic coefficients) are governed by a time-periodic DDE, and its stability depends on the spectral radius $|\lambda_{\max}|$ (i.e., the eigenvalue with largest magnitude) of the Floquet transition matrix (FTM), obtained using Floquet theory. The time-periodic DDE is stable only if $|\lambda_{\max}| < 1$. Thus, a primary objective of closed-loop control of a TDS is to ensure that $|\lambda_{\max}|$ remains less than 1. State-of-the-art methods to analyze the stability of time-periodic DDEs include Galerkin approximations [6, 15, 16],

direct numerical simulation [17, 18], semi-discretization [19, 20], full-discretization [21, 22], and Lyapunov functions [23, 24]. The difficulties associated with constructing the Lyapunov functions to determine the stability of TDS with time-periodic delays has been demonstrated by Liu and Liao [23] and Jiang et al. [24]. Numerical tools, such as the MATLAB® DDE-BIFTOOL package for bifurcation analysis [25], can alleviate much of the computational burden associated with simulating and analyzing DDE systems.

Very limited literature exists on the stabilization and control of DDEs with time-periodic delays. However, some strategies have been reported for DDEs with time-periodic coefficients, including optimization-based [26–29] and non-optimization-based [29–31] approaches. Butcher and Mann [26] used the Chebyshev polynomial expansion method to design delayed-state-feedback controllers for periodic TDS. Butcher et al. [28] used the Chebyshev spectral continuous-time approximation (CSCTA) and reduced Lyapunov–Floquet transformation to transform DDEs with time-periodic coefficients into systems of constant-coefficient ODEs. By effectively removing the delay and periodic coefficients, a closed-loop linear feedback controller could then be designed using traditional design tools for linear time-invariant systems. Zhang and Sun [27] designed an optimal proportional–integral–derivative feedback controller for a periodic linear time-delay system by minimizing the magnitude of the largest eigenvalue. Nazari et al. [29] developed three strategies to design controllers for linear periodic TDS. In the first strategy, a finite-dimensional monodromy operator was obtained using the Chebyshev collocation method; an optimal set of control gains was then obtained based on the minimum spectral radius. In the second strategy, the time-periodic DDE was transformed into a finite system of ODEs using the CSCTA technique. A cost function was then minimized using the linear–quadratic regulator (LQR) control method by directly solving the time-periodic Riccati equation backwards in time. In the third strategy, optimal control gains were obtained using CSCTA and the reduced Lyapunov–Floquet transformation in conjunction with either pole placement or LQR control. Ma et al. [30] used

shifted Chebyshev polynomials and Floquet theory to design a delayed-state-feedback controller for linear time-periodic TDS using a symbolic approach. The main limitation of this method is the size of the symbolic system that can be handled. Later, Ma et al. [31] proposed a symbolic method using Floquet theory for delayed-state-feedback controller design for linear time-periodic TDS. This method first constructs a finite-dimensional symbolic closed-loop monodromy matrix, then uses it in conjunction with the Routh–Hurwitz stability criterion to design constant-gain and periodic-gain delayed-state-feedback controllers. Very recently, Borgioli et al. [32] studied the stability robustness of linear DDE systems with time-periodic coefficients by computing the effect of perturbations in system parameters on the Floquet multipliers.

In this work, we consider the control of TDS with time-periodic delays by first obtaining a system of time-periodic ODEs. Our main focus is to enhance the delay tolerance of the system which, to the best of our knowledge, has not been considered in the literature. To design the controller, we must first analyze the stability of the periodic TDS. We use the Galerkin approximation method to determine the stability characteristics of periodic TDS, the efficacy of which has been demonstrated previously [6,15,16]. However, unique to this work, we consider two formulation strategies for the Galerkin method. In the first strategy, we convert the second-order time-periodic DDE into a time-periodic partial differential equation (PDE) along with boundary conditions. (Due to the presence of the time-periodic terms, the boundary conditions are also time-periodic.) The second-order PDE is then converted into a system of second-order time-periodic ODEs, and finally into a system of first-order time-periodic ODEs. We refer to this strategy as the "second-order Galerkin" method. In the second strategy, the second-order time-periodic DDE is converted into state-space form (i.e., into two first-order time-periodic DDEs), then into a system of first-order time-periodic PDEs, and finally into a system of first-order time-periodic ODEs. We refer to this strategy as the "first-order Galerkin" method. It was observed by Sadath and Vyasarayani [33] that the second-order Galerkin method results in an approximating ODE system with spurious Floquet multipliers.

The spurious Floquet multipliers do not influence the stability of the system, but they do pose practical challenges if one wishes to apply pole-placement techniques to stabilize the system. We propose an optimization-based framework combined with the Galerkin approximation method to perform pole placement, where the objective is to reduce the spectral radius $|\lambda_{\max}|$ of the FTM to a value less than 1. Finally, we perform experimental validation of the proposed approach, since very limited literature exists on validating stabilization techniques for TDS with time-periodic delays. Portions of this work appear in the Ph.D. thesis of Kandala [34].

The remainder of the paper is organized as follows. Section 2 describes the optimization problem. In Sec. 3, we provide a detailed description of how to find the stability regions of time-periodic DDEs, using both the second-order and first-order Galerkin formulation methods. In Sec. 4, we use a delayed Mathieu equation to demonstrate the existence of spurious Floquet multipliers when the second-order Galerkin method is used. We also highlight the limitations of using stability charts when many system parameters must be optimized. In Sec. 5, the proposed approach is applied to stabilize a rotary inverted pendulum apparatus with inherent sensing delays as well as additional time-periodic delays that are introduced deliberately. Finally, the conclusions drawn from this study are summarized in Sec. 6.

2 Pole Placement for Time-Periodic DDEs

The eigenvalues of time-periodic DDEs do not exist explicitly; for this reason, we use Floquet theory and study the spectral radius $|\lambda_{\max}|$ of the FTM. The spectral radius has a direct relationship to the stability characteristics of time-periodic systems. The proposed pole-placement technique described in this section can be used to stabilize single-input single-output systems as well as multiple-input multiple-output systems.

Consider the following system of DDEs, represented here in state-space form:

$$\dot{\mathbf{x}}(t) + \mathbf{A}\mathbf{x}(t) + \sum_{q=1}^{m} \mathbf{B}_q u_q(t - \tau_q(t)) = \mathbf{0}, \tag{1a}$$

$$u_q(t - \tau_q(t)) = \mathbf{K}_q^{\mathrm{T}} \mathbf{x}(t - \tau_q(t)), \quad q = 1, 2, \ldots, m, \tag{1b}$$

where $\mathbf{x}(t) \triangleq [x_1(t), x_2(t), \ldots, x_P(t)]^{\mathrm{T}}$ is the state vector, $\mathbf{u}(t) \triangleq [u_1(t), u_2(t), \ldots, u_m(t)]^{\mathrm{T}}$ is the control vector, $\mathbf{A} \in \mathbb{R}^{P \times P}$, $\mathbf{B}_q \in \mathbb{R}^{P \times 1}$, $\mathbf{K}_q \in \mathbb{R}^{P \times 1}$, and the time-periodic delays are $\tau_q(t) > 0$. Given $\mathbf{A}$, $\mathbf{B}_q$, and delays $\tau_q(t)$, the objective is to determine feedback gains $\mathbf{K}_q$ that stabilize the system (i.e., where all Floquet multipliers are less than 1). The gains $\mathbf{K}_q$ are determined by minimizing the following objective function:

$$J = \Big(|\lambda_{\max}(\mathbf{K}_q)| - \alpha \Big)^2, \tag{2}$$

where $|\lambda_{\max}|$ is the spectral radius of the FTM (described in more detail in Sec. 3), which is a function of the feedback gains $\mathbf{K}_q$; $0 \leq \alpha \leq 1$ is a parameter that specifies the desired spectral radius. Thus, it is necessary to determine $|\lambda_{\max}|$ of the FTM in order to find the optimal feedback gain matrix $\mathbf{K}_q^*$. Although not used in this work, constraints can be introduced into this optimization problem to reflect hardware limitations, power use requirements, a desired time-delay stability margin, or other practical constraints.

3 Mathematical Modeling

In this section, we present the Galerkin approximation method for systems governed by a second-order DDE with time-periodic delays. Our formulation applies to systems of any dimension (Eq. (1)), but for clarity of presentation we use the following scalar second-order DDE here:

$$\ddot{x}(t) + a_1 \dot{x}(t) + a_2 x(t) + \sum_{\rho=1}^{n} b_\rho \dot{x}(t - \tau_\rho(t)) + \sum_{q=1}^{m} c_q x(t - \tau_{n+q}(t)) = 0, \tag{3}$$

where $x(t)$ is the system state vector, $\dot{x}(t)$ and $\ddot{x}(t)$ are its time derivatives, $\mathbf{a} \in \mathbb{R}^2$, $\mathbf{b} \in \mathbb{R}^n$, $\mathbf{c} \in \mathbb{R}^m$, and delays $\tau_i(t) \geq 0$ for $i = 1, 2, \ldots, n+m$. Equation (3) is said to be a DDE with constant or discrete delays if all $\tau_i(t)$ are constant; if at least one $\tau_i(t)$ follows a periodic trajectory, then Eq. (3) is said to be a DDE with time-periodic delays. The time-periodic delays are assumed to have a fundamental time-period of T. Since we consider linear stability and pole placement in this work, the initial conditions are immaterial (as explained below). We convert infinite-dimensional second-order DDEs with time-periodic delays (Eq. (3)) into finite-dimensional systems of time-periodic ODEs using the Galerkin approximation method. Below, we describe two possible strategies for applying the Galerkin method.

3.1 Second-order Galerkin method

In this formulation, the second-order DDE with time-periodic delays is first converted into a second-order time-periodic PDE; the PDE is then converted into a system of second-order time-periodic ODEs which are finally written in first-order form. We briefly outline the formulation here; further detail can be found in Sadath and Vyasarayani [33]. First, consider the following transformation:

$$y(s,t) = x(t + \bar{\tau}(t)s), \quad -1 \leq s \leq 0, \quad t \geq 0. \tag{4}$$

Differentiating Eq. (4) with respect to time t and, separately, with respect to s reveals the following relation:

$$\frac{\partial y(s,t)}{\partial t} = \frac{1}{\bar{\tau}(t)} \frac{\partial y(s,t)}{\partial s} + \frac{\dot{\bar{\tau}}(t)}{\bar{\tau}(t)} \frac{s \partial y(s,t)}{\partial s}, \quad -1 \leq s \leq 0, \quad t \geq 0. \tag{5}$$

Now differentiating Eq. (5) with respect to t results in a second-order PDE:

$$\begin{aligned} \frac{\partial^2 y(s,t)}{\partial t^2} = & \frac{1}{\bar{\tau}(t)} \frac{\partial^2 y(s,t)}{\partial t \partial s} - \frac{\dot{\bar{\tau}}(t)}{\bar{\tau}^2(t)} \frac{\partial y(s,t)}{\partial s} \\ & + \frac{\dot{\bar{\tau}}(t)}{\bar{\tau}(t)} \frac{s \partial^2 y(s,t)}{\partial t \partial s} + \left[\frac{\bar{\tau}(t) \ddot{\bar{\tau}}(t) - \dot{\bar{\tau}}^2(t)}{\bar{\tau}^2(t)} \right] \frac{s \partial y(s,t)}{\partial s}. \end{aligned} \tag{6}$$

Thus, the DDE (Eq. (3)) has been re-cast as a PDE. Boundary conditions for Eq. (6) are obtained by substituting the transformation given by Eq. (4) into Eq. (3):

$$\left.\frac{\partial^2 y(s,t)}{\partial t^2}\right|_{s=0} + a_1 \left.\frac{\partial y(s,t)}{\partial t}\right|_{s=0} + a_2 y(0,t) + \sum_{\rho=1}^{n} b_\rho \left.\frac{\partial y(s,t)}{\partial t}\right|_{s=-\tau_\rho(t)/\bar{\tau}(t)} + \sum_{q=1}^{m} c_q y\left(-\frac{\tau_{n+q}(t)}{\bar{\tau}(t)}, t\right) = 0. \tag{7}$$

Briefly, the formulation concludes as follows. We assume a series solution and retain the first N terms (determined through a convergence analysis):

$$y(s,t) = \sum_{i=1}^{\infty} \phi_i(s)\eta_i(t) \approx \sum_{i=1}^{N} \phi_i(s)\eta_i(t) = \boldsymbol{\phi}^{\mathrm{T}}(s)\boldsymbol{\eta}(t), \tag{8}$$

where $\boldsymbol{\phi}(s) \triangleq [\phi_1(s), \phi_2(s), \ldots, \phi_N(s)]^{\mathrm{T}}$ and $\boldsymbol{\eta}(t) \triangleq [\eta_1(t), \eta_2(t), \ldots, \eta_N(t)]^{\mathrm{T}}$ are the vectors of basis functions and coordinates, respectively. We substitute the truncated series solution into Eq. (6), pre-multiply by $\boldsymbol{\phi}(s)$, and integrate over the domain $s \in [-1, 0]$ to obtain the following system of second-order time-periodic ODEs:

$$\mathbf{M}\ddot{\boldsymbol{\eta}}(t) = \left(\frac{1}{\bar{\tau}(t)}\mathbf{C} + \frac{\dot{\bar{\tau}}(t)}{\bar{\tau}(t)}\mathbf{D}\right)\dot{\boldsymbol{\eta}}(t) + \left(\frac{-\dot{\bar{\tau}}(t)}{\bar{\tau}^2(t)}\mathbf{C} + \frac{\bar{\tau}(t)\ddot{\bar{\tau}}(t) - \dot{\bar{\tau}}^2(t)}{\bar{\tau}^2(t)}\mathbf{D}\right)\boldsymbol{\eta}(t). \tag{9}$$

Matrices $\mathbf{M}$, $\mathbf{C}$, and $\mathbf{D}$ are defined as follows:

$$\mathbf{M} \triangleq \int_{-1}^{0} \boldsymbol{\phi}(s)\boldsymbol{\phi}^{\mathrm{T}}(s)\, ds, \quad \mathbf{C} \triangleq \int_{-1}^{0} \boldsymbol{\phi}(s)\boldsymbol{\phi}'(s)^{\mathrm{T}}\, ds, \quad \mathbf{D} \triangleq \int_{-1}^{0} s\boldsymbol{\phi}(s)\boldsymbol{\phi}'(s)^{\mathrm{T}}\, ds, \tag{10}$$

where $\boldsymbol{\phi}'(s)$ denotes the derivative of $\boldsymbol{\phi}(s)$ with respect to s. For simplicity of notation, we define the following:

$$\widehat{\mathbf{C}} = \frac{1}{\bar{\tau}(t)}\mathbf{C} + \frac{\dot{\bar{\tau}}(t)}{\bar{\tau}(t)}\mathbf{D}, \tag{11a}$$

$$\widehat{\mathbf{D}} = \frac{-\dot{\bar{\tau}}(t)}{\bar{\tau}^2(t)}\mathbf{C} + \frac{\bar{\tau}(t)\ddot{\bar{\tau}}(t) - \dot{\bar{\tau}}^2(t)}{\bar{\tau}^2(t)}\mathbf{D}, \tag{11b}$$

whereupon Eq. (9) can be written as

$$\mathbf{M}\ddot{\boldsymbol{\eta}}(t) = \widehat{\mathbf{C}}\dot{\boldsymbol{\eta}}(t) + \widehat{\mathbf{D}}\boldsymbol{\eta}(t). \tag{12}$$

The boundary conditions for the DDE given by Eq. (3) are as follows:

$$\mathbf{m}\ddot{\boldsymbol{\eta}}(t) = \mathbf{c}\dot{\boldsymbol{\eta}}(t) + \mathbf{d}\boldsymbol{\eta}(t), \tag{13}$$

where $\mathbf{m}$, $\mathbf{c}$, and $\mathbf{d}$ are given by the following:

$$\mathbf{m} = \boldsymbol{\phi}^{\mathrm{T}}(0), \tag{14a}$$

$$\mathbf{c} = -a_1\boldsymbol{\phi}^{\mathrm{T}}(0) - \sum_{\rho=1}^{n} b_\rho \boldsymbol{\phi}^{\mathrm{T}}\left(\frac{-\tau_\rho(t)}{\bar{\tau}(t)}\right), \tag{14b}$$

$$\mathbf{d} = -a_2\boldsymbol{\phi}^{\mathrm{T}}(0) - \sum_{q=1}^{m} c_q \boldsymbol{\phi}^{\mathrm{T}}\left(\frac{-\tau_{n+q}(t)}{\bar{\tau}(t)}\right). \tag{14c}$$

The boundary conditions can be incorporated into Eq. (12) using the spectral Tau method [35, 36], ultimately resulting in the following system of ODEs:

$$\begin{bmatrix}\overline{\mathbf{M}}\\ \mathbf{m}\end{bmatrix}\ddot{\boldsymbol{\eta}}(t) = \begin{bmatrix}\overline{\mathbf{C}}\\ \mathbf{c}\end{bmatrix}\dot{\boldsymbol{\eta}}(t) + \begin{bmatrix}\overline{\mathbf{D}}\\ \mathbf{d}\end{bmatrix}\boldsymbol{\eta}(t), \tag{15}$$

where matrices $\overline{\mathbf{M}}$, $\overline{\mathbf{C}}$, and $\overline{\mathbf{D}}$ are the truncated matrices of size $N-1\times N$ obtained upon removing the last row from matrices $\mathbf{M}$, $\widehat{\mathbf{C}}$, and $\widehat{\mathbf{D}}$, respectively. Defining a state vector $\mathbf{z}(t) \triangleq \left[\boldsymbol{\eta}^{\mathrm{T}}(t), \dot{\boldsymbol{\eta}}^{\mathrm{T}}(t)\right]^{\mathrm{T}} \in \mathbb{R}^{2N}$, Eq. (15) can be rewritten as follows:

$$\dot{\mathbf{z}}(t) = \begin{bmatrix}\mathbf{0} & \mathbf{I}\\ \widetilde{\mathbf{M}}^{-1}\widetilde{\mathbf{D}}(t) & \widetilde{\mathbf{M}}^{-1}\widetilde{\mathbf{C}}(t)\end{bmatrix}\mathbf{z}(t) = \mathbf{G}_{\mathrm{so}}(t)\mathbf{z}(t), \tag{16}$$

where $\widetilde{\mathbf{M}} = \begin{bmatrix}\overline{\mathbf{M}}\\ \mathbf{m}\end{bmatrix}$, $\widetilde{\mathbf{C}} = \begin{bmatrix}\overline{\mathbf{C}}\\ \mathbf{c}\end{bmatrix}$, $\widetilde{\mathbf{D}} = \begin{bmatrix}\overline{\mathbf{D}}\\ \mathbf{d}\end{bmatrix}$, and $\mathbf{I}$ is an identity matrix.

Matrix $\mathbf{G}_{\mathrm{so}}(t)$ is periodic (with period T), thus Floquet theory is used to determine the stability of Eq. (16). The Floquet transition matrix (FTM) $\boldsymbol{\Phi}(T)$ is defined as follows:

$$\mathbf{r}(T) = \boldsymbol{\Phi}(T)\mathbf{r}(0). \tag{17}$$

Thus, the FTM describes a mapping of an initial state ($\mathbf{r}(0)$) onto the state one period later ($\mathbf{r}(T)$). The FTM is obtained by integrating the following equation for $t \in [0, T]$:

$$\dot{\mathbf{\Phi}}(t) = \mathbf{G}_{\mathrm{so}}(t)\mathbf{\Phi}(t), \tag{18}$$

using $\mathbf{\Phi}(0) = \mathbf{I}$ as the initial conditions. We refer to the largest eigenvalue (in absolute value) of the FTM ($|\lambda_{\max}|$) as its *spectral radius*; Eq. (16) is stable only if $|\lambda_{\max}| < 1$.

3.2 First-order Galerkin method

In this formulation, the second-order DDE with time-periodic delays is first converted into a system of first-order DDEs with time-periodic delays. We then obtain a system of first-order PDEs with time-periodic coefficients and, finally, a system of first-order time-periodic ODEs. We begin by defining state vector $\mathbf{w} \triangleq [x(t), \dot{x}(t)]^{\mathrm{T}}$ and rewriting Eq. (3) as follows:

$$\dot{\mathbf{w}}(t) = \mathbf{A}\mathbf{w}(t) + \sum_{\rho=1}^{n} \mathbf{B}_\rho \mathbf{w}(t - \tau_\rho(t)) + \sum_{q=1}^{m} \mathbf{Q}_q \mathbf{w}(t - \tau_{n+q}(t)), \tag{19}$$

where matrices $\mathbf{A}$, $\mathbf{B}_\rho$, and $\mathbf{Q}_q$ are given as follows:

$$\mathbf{A} = \begin{bmatrix} 0 & 1 \\ -a_2 & -a_1 \end{bmatrix}, \quad \mathbf{B}_\rho = \begin{bmatrix} 0 & 0 \\ 0 & -b_\rho \end{bmatrix}, \quad \mathbf{Q}_q = \begin{bmatrix} 0 & 0 \\ -c_q & 0 \end{bmatrix}. \tag{20}$$

Next, we introduce the following transformation (analogous to Eq. (4)):

$$\mathbf{y}(s, t) = \mathbf{w}(t + \bar{\tau}(t)s), \quad -1 \le s \le 0, \quad t \ge 0. \tag{21}$$

Differentiating Eq. (21) with respect to t and, separately, with respect to s, we obtain the following relation (analogous to Eq. (5)):

$$\frac{\partial \mathbf{y}(s,t)}{\partial t} = \frac{1}{\bar{\tau}(t)} \frac{\partial \mathbf{y}(s,t)}{\partial s} + \frac{\dot{\bar{\tau}}(t)}{\bar{\tau}(t)} \frac{s \partial \mathbf{y}(s,t)}{\partial s}, \quad -1 \le s \le 0, \quad t \ge 0. \tag{22}$$

Boundary conditions for Eq. (3) are obtained by substituting Eq. (21) into Eq. (19):

$$\left.\frac{\partial \mathbf{y}(s,t)}{\partial t}\right|_{s=0} = \mathbf{A}\mathbf{y}(0,t) + \sum_{\rho=1}^{n} \mathbf{B}_\rho \mathbf{y}\left(\frac{-\tau_\rho(t)}{\bar{\tau}(t)}, t\right) + \sum_{q=1}^{m} \mathbf{Q}_q \mathbf{y}\left(\frac{-\tau_{n+q}(t)}{\bar{\tau}(t)}, t\right). \tag{23}$$

Thus, the original DDE (Eq. (3)) is converted into an equivalent system of first-order PDEs (Eq. (22)) with boundary conditions given by Eq. (23). A system of first-order ODEs is now obtained by assuming a series solution and retaining the first N terms:

$$y_i(s,t) = \sum_{j=1}^{\infty} \phi_j(s) z_{ij}(t) \approx \sum_{j=1}^{N} \phi_j(s) z_{ij}(t) = \boldsymbol{\phi}^{\mathrm{T}}(s)\mathbf{z}_i(t), \quad i = 1, 2, \tag{24}$$

where $\boldsymbol{\phi}(s) \triangleq [\phi_1(s), \phi_2(s), \ldots, \phi_N(s)]^{\mathrm{T}}$ and $\mathbf{z}_i(t) \triangleq [z_{i1}(t), z_{i2}(t), \ldots, z_{iN}(t)]^{\mathrm{T}}$ are the vectors of basis functions and coordinates, respectively. We define $\boldsymbol{\Psi}(s) \in \mathbb{R}^{2N\times 2}$ and $\boldsymbol{\beta}(t) \in \mathbb{R}^{2N}$ as follows:

$$\boldsymbol{\Psi}(s) = \begin{bmatrix} \boldsymbol{\phi}(s) & \mathbf{0} \\ \mathbf{0} & \boldsymbol{\phi}(s) \end{bmatrix}, \quad \boldsymbol{\beta}(t) = \begin{Bmatrix} \mathbf{z}_1(t) \\ \mathbf{z}_2(t) \end{Bmatrix}, \tag{25}$$

whereupon Eq. (24) can be written as follows:

$$\mathbf{y}(s,t) = \boldsymbol{\Psi}^{\mathrm{T}}(s)\boldsymbol{\beta}(t). \tag{26}$$

Substituting Eq. (26) into Eq. (22), we obtain the following:

$$\boldsymbol{\Psi}^{\mathrm{T}}(s)\dot{\boldsymbol{\beta}}(t) = \left[\frac{1}{\bar{\tau}(t)} + \frac{s\dot{\bar{\tau}}(t)}{\bar{\tau}(t)}\right] \boldsymbol{\Psi}'(s)^{\mathrm{T}}\boldsymbol{\beta}(t). \tag{27}$$

Pre-multiplying Eq. (27) by $\boldsymbol{\Psi}(s)$ and integrating over the domain $s \in [-1, 0]$ produces a system of first-order time-periodic ODEs:

$$\mathbf{P}\dot{\boldsymbol{\beta}}(t) = \left[\frac{1}{\bar{\tau}(t)}\mathbf{R} + \frac{\dot{\bar{\tau}}(t)}{\bar{\tau}(t)}\mathbf{S}\right] \boldsymbol{\beta}(t), \tag{28}$$

where matrices $\mathbf{P}$, $\mathbf{R}$, and $\mathbf{S}$ are square, block-diagonal, and of dimension $2N$:

$$\mathbf{P} = \begin{bmatrix} \mathbf{P}^{(1)} & \mathbf{0} \\ \mathbf{0} & \mathbf{P}^{(2)} \end{bmatrix}, \quad \mathbf{R} = \begin{bmatrix} \mathbf{R}^{(1)} & \mathbf{0} \\ \mathbf{0} & \mathbf{R}^{(2)} \end{bmatrix}, \quad \mathbf{S} = \begin{bmatrix} \mathbf{S}^{(1)} & \mathbf{0} \\ \mathbf{0} & \mathbf{S}^{(2)} \end{bmatrix}. \tag{29}$$

Submatrices $\mathbf{P}^{(k)}$, $\mathbf{R}^{(k)}$, and $\mathbf{S}^{(k)}$ are defined as follows for $k = 1, 2$:

$$\mathbf{P}^{(k)} \triangleq \int_{-1}^{0} \boldsymbol{\phi}_i(s)\boldsymbol{\phi}_i^{\mathrm{T}}(s)\, ds, \quad \mathbf{R}^{(k)} \triangleq \int_{-1}^{0} \boldsymbol{\phi}_i(s)\boldsymbol{\phi}_i'(s)^{\mathrm{T}}\, ds, \quad \mathbf{S}^{(k)} \triangleq \int_{-1}^{0} s\boldsymbol{\phi}_i(s)\boldsymbol{\phi}_i'(s)^{\mathrm{T}}\, ds. \tag{30}$$

The matrix of boundary conditions is obtained by substituting the series solution (Eq. (24)) into Eq. (23):

$$\mathbf{\Psi}^{\mathrm{T}}(0)\dot{\boldsymbol{\beta}}(t) = \left[\mathbf{A}\mathbf{\Psi}^{\mathrm{T}}(0) + \sum_{\rho=1}^{n}\mathbf{B}_{\rho}\mathbf{\Psi}^{\mathrm{T}}\left(\frac{-\tau_{\rho}(t)}{\bar{\tau}(t)}\right) + \sum_{q=1}^{m}\mathbf{Q}_{q}\mathbf{\Psi}^{\mathrm{T}}\left(\frac{-\tau_{n+q}(t)}{\bar{\tau}(t)}\right)\right]\boldsymbol{\beta}(t). \tag{31}$$

Equations (28) and (31) can be combined as follows:

$$\mathbf{U}\dot{\boldsymbol{\beta}}(t) = \mathbf{V}(t)\boldsymbol{\beta}(t) \tag{32a}$$

$$\Rightarrow \quad \dot{\boldsymbol{\beta}}(t) = \mathbf{U}^{-1}\mathbf{V}(t)\boldsymbol{\beta}(t) \triangleq \mathbf{G}_{\mathrm{fo}}(t)\boldsymbol{\beta}(t), \tag{32b}$$

where $\mathbf{U}$ and $\mathbf{V}$ are square matrices of dimension $2N$ and are obtained by replacing the N-th and $2N$-th rows of Eq. (28) with the first and second rows of Eq. (31), respectively.

Matrix $\mathbf{G}_{\mathrm{fo}}(t)$ is periodic (with period T); thus, as above for the second-order Galerkin method, we use Floquet theory to determine the stability of Eq. (32). In this case, the FTM $\mathbf{\Phi}(T)$ is defined as follows:

$$\boldsymbol{\beta}(T) = \mathbf{\Phi}(T)\boldsymbol{\beta}(0). \tag{33}$$

Once again, the FTM describes a mapping of an initial state ($\boldsymbol{\beta}(0)$) onto the state one period later ($\boldsymbol{\beta}(T)$). The FTM is obtained by integrating the following equation for $t \in [0, T]$:

$$\dot{\mathbf{\Phi}}(t) = \mathbf{G}_{\mathrm{fo}}(t)\mathbf{\Phi}(t), \tag{34}$$

using $\mathbf{\Phi}(0) = \mathbf{I}$ as the initial conditions. As before, Eq. (32) is stable only if the spectral radius of the FTM ($|\lambda_{\max}|$) is less than 1.

3.3 Basis functions

In spectral methods, one must select an appropriate set of basis functions $\boldsymbol{\phi}(s)$ to obtain the solution of the approximating ODE system. In this work, we use shifted Legendre polynomials since they

have been shown to have good convergence properties [35]:

$$\phi_1(s) = 1, \tag{35a}$$

$$\phi_2(s) = 1 + \frac{2s}{\bar{\tau}}, \tag{35b}$$

$$\phi_k(s) = \frac{(2k-3)\,\phi_2(s)\phi_{k-1}(s) - (k-2)\,\phi_{k-2}(s)}{k-1}, \quad k \geq 3. \tag{35c}$$

Using these basis functions, matrices $\mathbf{M}$, $\widehat{\mathbf{C}}$, and $\widehat{\mathbf{D}}$ in the second-order formulation (Eq. (12)) and matrices $\mathbf{P}$, $\mathbf{R}$, and $\mathbf{S}$ in the first-order formulation (Eq. (29)) can be expressed in closed form as follows [33]:

$$\mathbf{M}_{ij} = \mathbf{P}_{ij}^{(k)} = \begin{cases} \frac{1}{2i-1}, & \text{if } i = j \\ 0, & \text{otherwise} \end{cases}, \tag{36a}$$

$$\mathbf{C}_{ij} = \mathbf{R}_{ij}^{(k)} = \begin{cases} 2, & \text{if } i+j \text{ is odd} \\ 0, & \text{otherwise} \end{cases}, \tag{36b}$$

$$\mathbf{D}_{ij} = \mathbf{S}_{ij}^{(k)} = \begin{cases} \frac{i-1}{2i-1}, & \text{if } i = j \\ (-1)^{i+j}, & \text{if } i < j \\ 0, & \text{otherwise} \end{cases}, \tag{36c}$$

where $i, j = 1, 2, \ldots, N$ and $k = 1, 2$.

4 Results and Discussion

In this section, we present two illustrative examples. In the first example, we use an example from the literature [2] to demonstrate the existence of spurious Floquet multipliers in the second-order Galerkin formulation. We then illustrate the limitations of using stability charts alone to determine suitable parameter values in a complicated system, motivating an optimization-based approach.

4.1 Delayed damped Mathieu equation

Consider the following delayed damped Mathieu equation, a second-order DDE [37]:

$$\ddot{x}(t) + c\dot{x}(t) + (\delta + \epsilon\cos(\omega t))\, x(t) = kx(t - \tau(t)), \tag{37}$$

with $c = \omega = 2$, $k = 1$, and time-periodic delay $\tau(t) = 0.6 + 0.2\cos(t)$. We use the second-order and first-order Galerkin formulations, each with $N = 10$ terms in the series solution, to convert the time-periodic DDE given by Eq. (37) into a system of time-periodic ODEs where $\mathbf{G}_{\text{so}}(t) \in \mathbb{R}^{20\times 20}$ (see Eq. (16)) and $\mathbf{G}_{\text{fo}}(t) \in \mathbb{R}^{20\times 20}$ (see Eq. (32b)). The Floquet multipliers obtained using the second-order Galerkin formulation are shown in Fig. 1(A) for $\delta = -1.5$ and $\epsilon = 4.17$, and in Fig. 1(B) for the same value of δ but with $\epsilon = 4.25$. We clearly see that the second-order formulation produces Floquet multipliers on the unit circle in each case. As shown in Fig. 2, the first-order formulation does not produce these spurious Floquet multipliers in either case. Note that the system is stable when $\epsilon = 4.17$ (Figs. 1(A) and 2(A)) and unstable when $\epsilon = 4.25$ (Figs. 1(B) and 2(B)). Notably, the second-order formulation is observed to produce spurious Floquet multipliers for both stable and unstable systems.

The stability chart for this system in the $[\delta, \epsilon]$ plane is shown in Fig. 3, generated using both the second-order and first-order formulations. The stability charts are generated by dividing the parameter space into a fine grid and computing the Floquet multipliers at each grid point. If all Floquet multipliers lie within the unit circle, the system is stable; otherwise, it is unstable. Note that the stability regions are identical, but that the stability contour cannot be obtained using the second-order formulation (Fig. 3(A)) due to the spurious Floquet multipliers. By contrast, the stability contour can be readily obtained using the first-order formulation (Fig. 3(B)). The first-order formulation would therefore be preferable for pole placement, where parameters δ and ϵ could be selected using Fig. 3(B) to achieve a desired spectral radius. The stability contour is also useful for identifying ranges of parameter values for which the system is stable but could

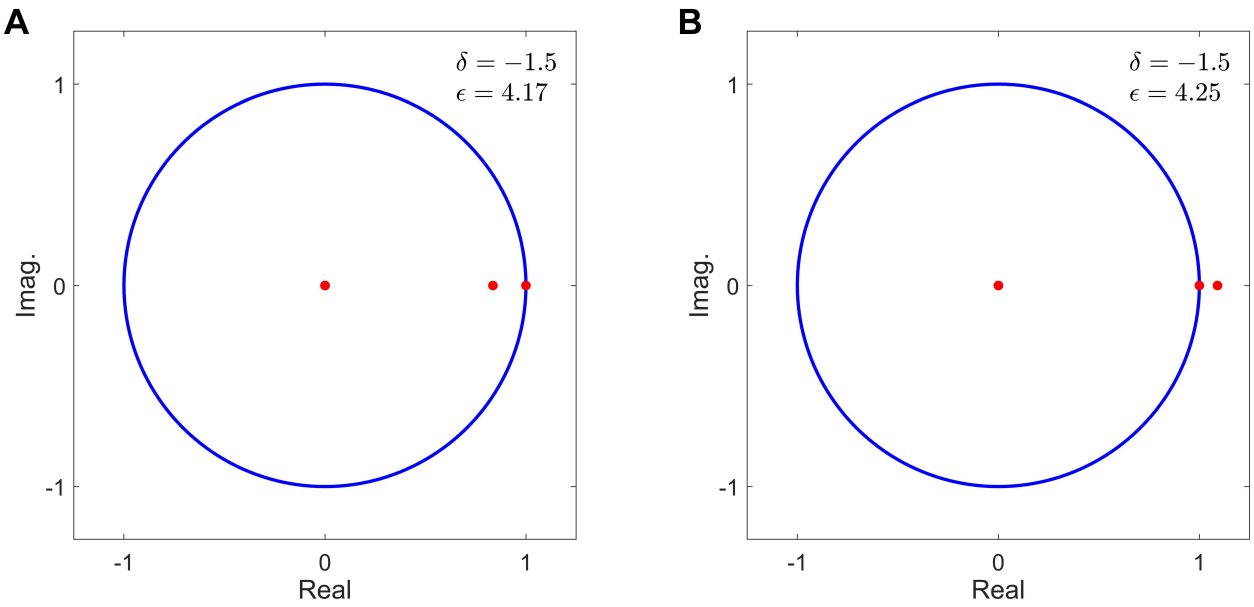

Figure 1: Floquet multipliers for the system given by Eq. (37) with $\delta = -1.5$, obtained using the *second-order* Galerkin formulation, for (A) $\epsilon = 4.17$ and (B) $\epsilon = 4.25$. Note that there are spurious Floquet multipliers at the point $(1, 0)$ in both cases.

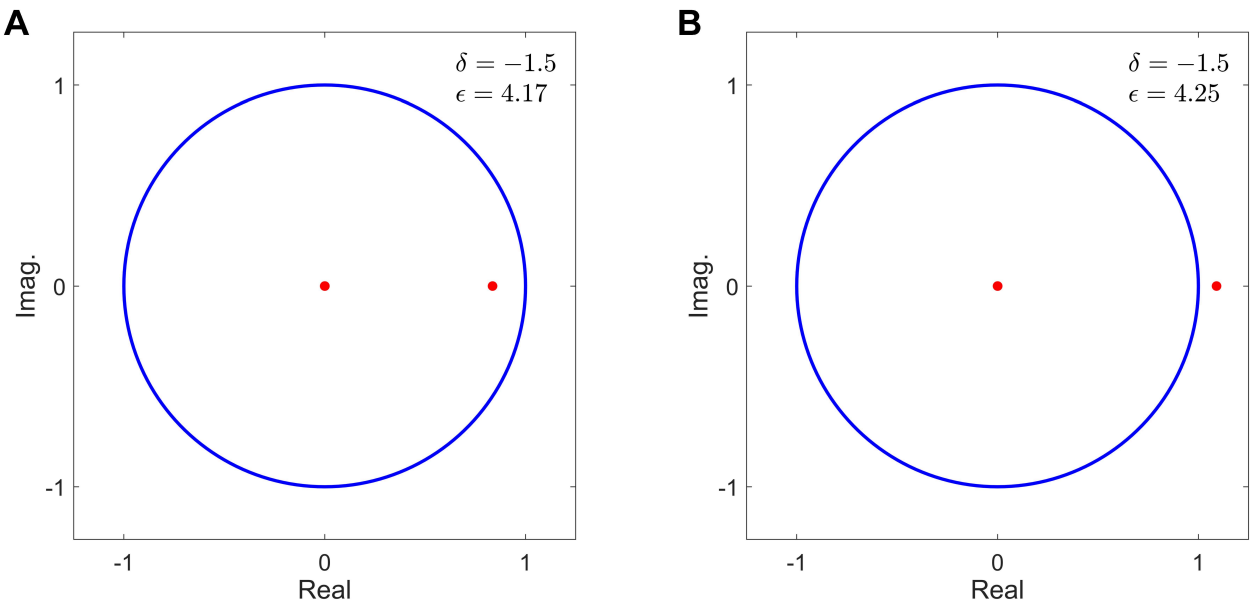

Figure 2: Floquet multipliers for the system given by Eq. (37) with $\delta = -1.5$, obtained using the *first-order* Galerkin formulation, for (A) $\epsilon = 4.17$ and (B) $\epsilon = 4.25$. Note that the spurious Floquet multipliers observed in Fig. 1 are absent.

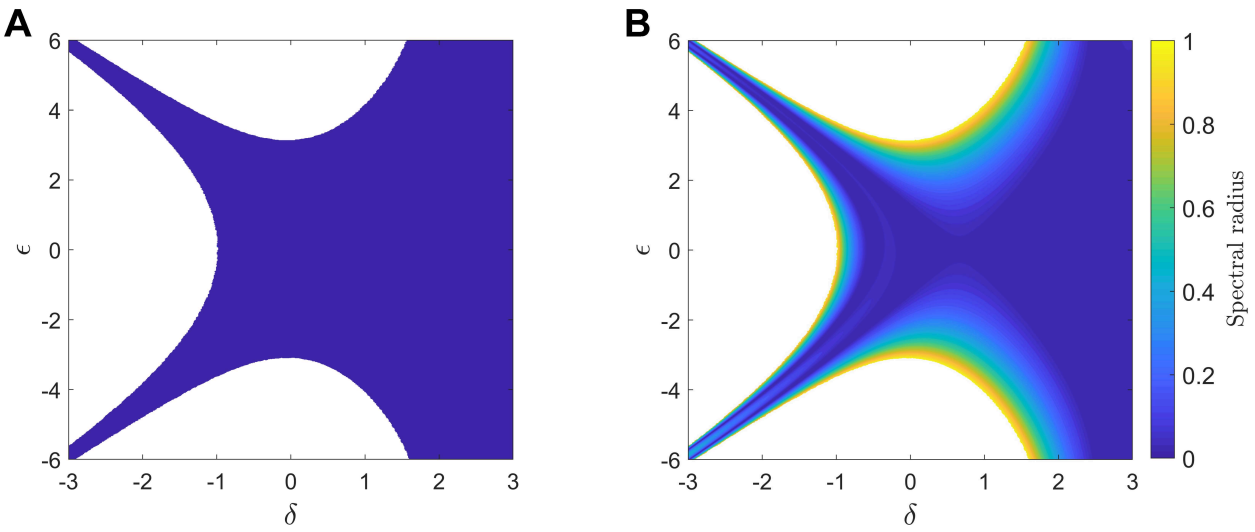

Figure 3: Stability chart for the system given by Eq. (37) in the $[\delta, \epsilon]$ plane, obtained using (A) the second-order Galerkin formulation and (B) the first-order Galerkin formulation. The stability regions are identical but only the first-order formulation provides the stability contour.

become unstable with small perturbations in the parameters. This first example demonstrates that the stability contour obtained using the first-order formulation can provide important insight into the control problem. We use the first-order formulation in the remainder of the paper.

4.2 First-order DDE with two time-periodic delays

Consider the following first-order time-periodic DDE [2]:

$$\dot{x}(t) - ax(t) - bx(t - \tau_1(t)) - cx(t - \tau_2(t)) = 0, \tag{38}$$

with time-periodic delays $\tau_1(t) = 0.6 - 0.4\sin(t)$ and $\tau_2(t) = 0.6 - 0.2\sin(t)$. We convert this time-periodic DDE into a system of time-periodic ODEs of the form given by Eq. (32b), with $N = 7$ terms in the series solution (Eq. (24)) and $\mathbf{G}_{\text{fo}}(t) \in \mathbb{R}^{14\times14}$. In this case, we have three parameters to tune: a, b, and c. The 3D stability chart in the $[a, b, c]$ space is shown in Fig. 4(A) for

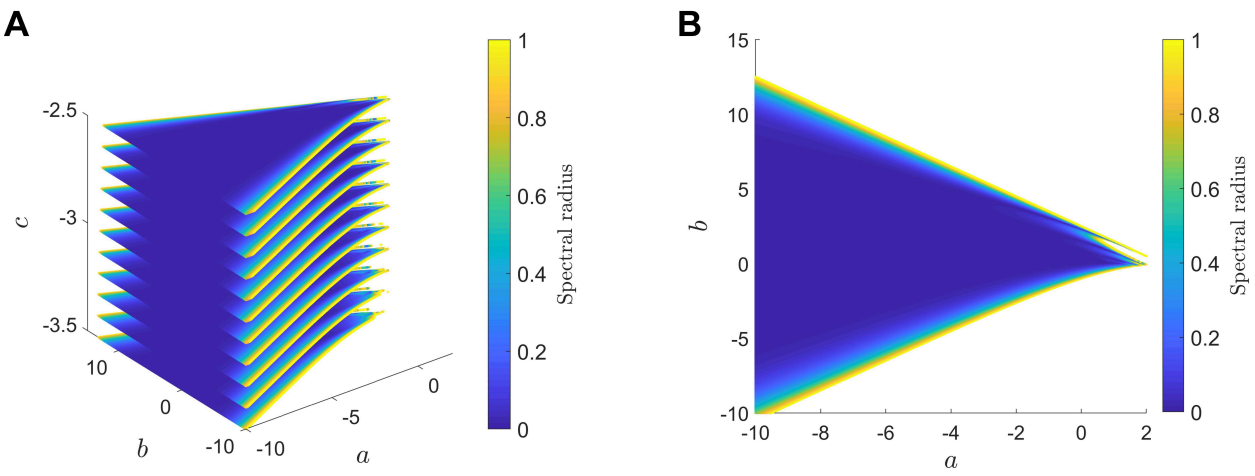

Figure 4: Stability contours for the system given by Eq. (38) shown (A) in the $[a, b, c]$ space and (B) in the $[a, b]$ plane with $c = -2.5$.

$a \in [-10, 2]$, $b \in [-10, 15]$, and $c \in [-3.5, -2.5]$, varying c in steps of 0.1; Fig. 4(B) shows only the topmost slice (i.e., where $c = -2.5$). As in the previous example, a series of stability contours could be used to identify suitable ranges of parameter values; however, note that the difficulty of this approach increases dramatically for systems with many parameters. For a more general approach, we propose an optimization-based framework to improve the closed-loop stability of time-delay systems, which we demonstrate in Sec. 5.

5 Experimental Validation

In this section, the proposed Galerkin approximation–based optimization framework is validated using the rotary inverted pendulum apparatus from Quanser (QUBE-Servo Rotary Servo Experiment, Quanser Inc., Markham, Ontario, Canada), shown in Fig. 5. The apparatus comprises a free-swinging rigid pendulum mounted to the end of a servo-driven rotary arm. The position of the arm is given by θ as it rotates about the vertical axis in the horizontal plane; the position of the

Figure 5: Rotary inverted pendulum apparatus, shown here with $\theta \approx 0^\circ$ and $\gamma \approx 180^\circ$.

pendulum is given by γ, where $\gamma = 0^\circ$ when the pendulum is hanging at rest and $\gamma = 180^\circ$ when it is inverted.

The linearized equations of motion for the rotary inverted pendulum system are as follows [38]:

$$\left(J_r + m_p \ell_r^2\right) \ddot{\theta}(t) - \tfrac{1}{2} m_p \ell_p \ell_r \ddot{\gamma}(t) = T(t) - B_r \dot{\theta}(t), \tag{39a}$$

$$\left(J_p + \tfrac{1}{4} m_p \ell_p^2\right) \ddot{\gamma}(t) - \tfrac{1}{2} m_p \ell_p \ell_r \ddot{\theta}(t) - \tfrac{1}{2} m_p \ell_p g \gamma(t) = -B_p \dot{\gamma}(t), \tag{39b}$$

where ℓ_p, m_p, and J_p are the length, mass, and moment of inertia of the pendulum with respect to its pivot point; ℓ_r is the length of the rotary arm; J_r is the equivalent moment of inertia acting on the servo shaft; B_p is the viscous damping about the pendulum's pivot; B_r is the viscous damping about the servo shaft; g is the gravitational acceleration; and $T(t)$ is the torque applied by the servo

to the rotary arm. The torque $T(t)$ is given by the following [38]:

$$T(t) = \frac{k_m}{R_m}\left(V_m(t) - k_m\dot{\theta}(t)\right), \tag{40}$$

where k_m is the DC motor back-electromotive force constant, R_m is the electrical resistance of the DC motor armature, and $V_m(t)$ is the input voltage (the control signal). Numerical values for these parameters are provided by Quanser [38] and are listed in Table 1. We can express the linearized equations of motion for the rotary inverted pendulum system (Eq. (39)) in state-space form as follows:

$$\dot{\mathbf{x}}(t) = \mathbf{A}\mathbf{x}(t) + \mathbf{B}u(t), \tag{41a}$$

$$u(t) = -\mathbf{K}^{\mathrm{T}}\mathbf{x}(t), \tag{41b}$$

where $\mathbf{x}(t) \triangleq \left[\theta(t), \gamma(t), \dot{\theta}(t), \dot{\gamma}(t)\right]^{\mathrm{T}}$ is the state vector, $u(t) \triangleq V_m(t)$ is the control input, and $\mathbf{A}$ and $\mathbf{B}$ are given as follows:

$$\mathbf{A} = \begin{bmatrix} 0 & 0 & 1 & 0 \\ 0 & 0 & 0 & 1 \\ 0 & 149.2751 & -0.0104 & 0 \\ 0 & 261.6091 & -0.0103 & 0 \end{bmatrix}, \qquad \mathbf{B} = \begin{Bmatrix} 0 \\ 0 \\ 49.7275 \\ 49.1493 \end{Bmatrix}. \tag{42}$$

The controller sampling frequency is 500 Hz, and thus the system has an inherent delay of 2 ms. We first consider controlling the system in its original form, without introducing any additional delays. Here, we use feedback gains $\mathbf{K} = [-2, 30, -2, 2.5]^{\mathrm{T}}$, which are provided by Quanser for the balance control exercise [39]. The steady-state response of the system is shown in Fig. 6. Note that the system is stable about its vertical equilibrium position ($\gamma = 180°$) and recovers when an external disturbance force is applied.

An additional sensing delay is now introduced. We use a time-periodic delay of the form

Table 1: Parameter values for the rotary inverted pendulum apparatus [38].

Parameter	Value	Units
ℓ_p	0.129	m
ℓ_r	0.085	m
m_p	0.024	kg
J_p	3.32820×10^{-5}	$\text{kg} \cdot \text{m}^2$
J_r	5.71979×10^{-5}	$\text{kg} \cdot \text{m}^2$
B_p	0	$\text{N} \cdot \text{m} \cdot \text{s} \cdot \text{rad}^{-1}$
B_r	0	$\text{N} \cdot \text{m} \cdot \text{s} \cdot \text{rad}^{-1}$
R_m	8.4	Ω
k_m	0.042	$\text{V} \cdot \text{s} \cdot \text{rad}^{-1}$
g	9.81	$\text{m} \cdot \text{s}^{-2}$

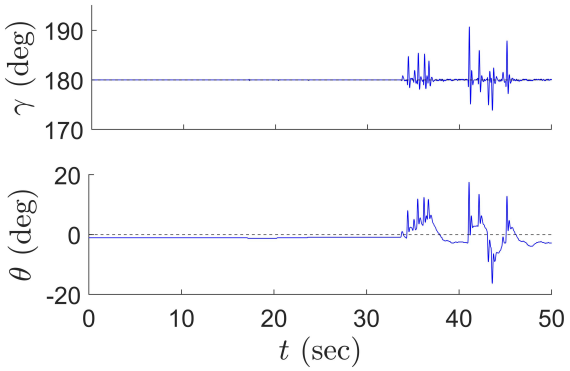

Figure 6: Stable response of the inverted pendulum (γ) and rotary arm (θ) with an inherent delay of 2 ms and feedback gains $\mathbf{K} = [-2, 30, -2, 2.5]^{\mathrm{T}}$. An external disturbance force is applied for $t \in [33, 47]$.

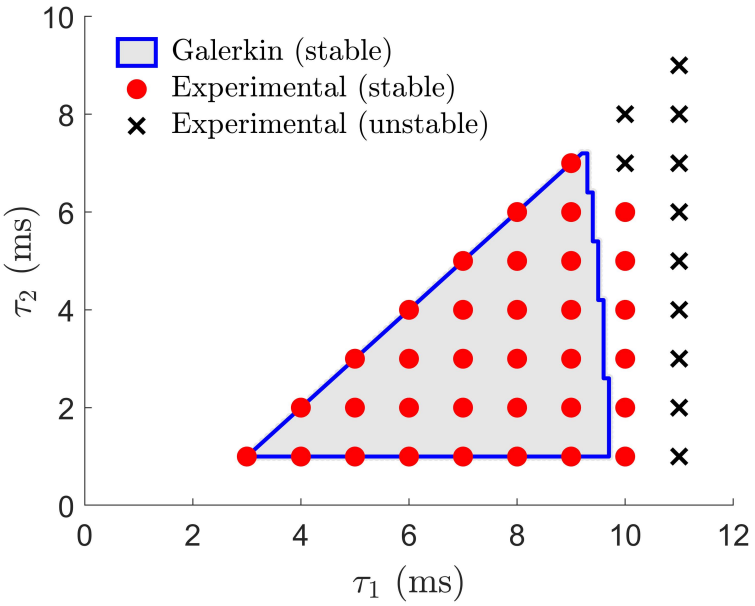

Figure 7: Stability chart of the rotary inverted pendulum system obtained numerically using the first-order Galerkin formulation (shaded region) and determined experimentally (circles indicate stable responses; crosses, unstable responses), using feedback gains $\mathbf{K} = [-2, 30, -2, 2.5]^{\mathrm{T}}$. The stability boundaries for increasing τ_1 are in good agreement.

$\tau(t) = \tau_1 + \tau_2 \sin(t)$, which results in the following state-space representation of the system:

$$\dot{\mathbf{x}}(t) = \mathbf{A}\mathbf{x}(t) + \mathbf{B}u(t - \tau(t)), \tag{43}$$

where matrix $\mathbf{A}$ and vector $\mathbf{B}$ are given by Eq. (42), $\tau_1 \geq 2$ ms, and $\tau_2 \leq \tau_1 - 2$ ms. These constraints on τ_1 and τ_2 account for the system's inherent delay of 2 ms (which cannot be removed) and ensure that the total delay is never negative. Figure 7 shows the stability chart in the $[\tau_1, \tau_2]$ plane, obtained using the first-order Galerkin formulation and the same feedback gains $\mathbf{K}$ as above. The shaded region indicates the combinations of τ_1 and τ_2 for which we anticipate the system will be stable (i.e., where the magnitude of the largest eigenvalue is less than 1).

Experimental validation is performed using the apparatus shown in Fig. 5. We introduce the time-periodic delay $\tau(t)$ defined above into the feedback controller and perform two sets of ex-

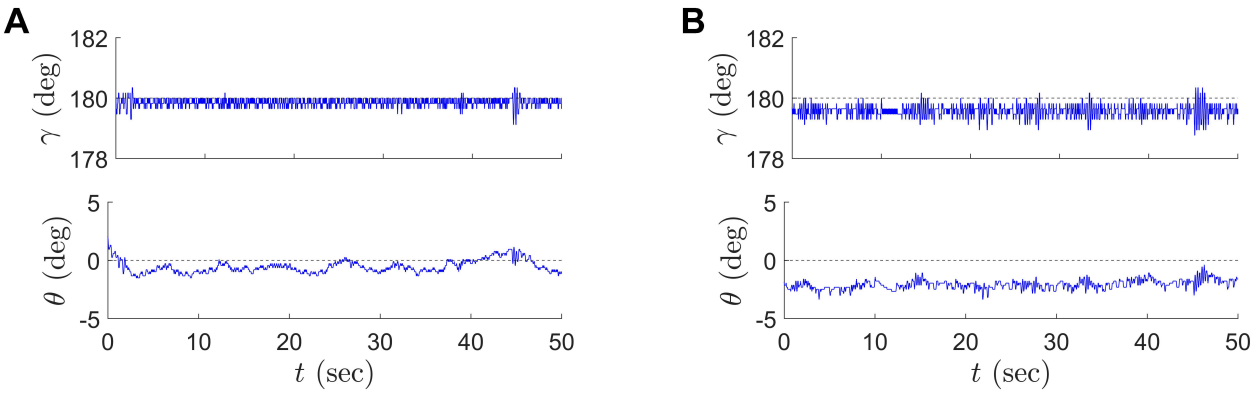

Figure 8: Stable response of the inverted pendulum (γ) and rotary arm (θ) using feedback gains $\mathbf{K} = [-2, 30, -2, 2.5]^{\mathrm{T}}$ with a time-periodic delay: (A) $\tau(t) = 10 + 5\sin(t)$ ms and (B) $\tau(t) = 10 + 6\sin(t)$ ms.

periments. In the first set of experiments, we consider several values of τ_1 and τ_2 using the same feedback gains as before, $\mathbf{K} = [-2, 30, -2, 2.5]^{\mathrm{T}}$. In Fig. 7, the points marked with circles are the combinations of τ_1 and τ_2 for which the physical system is stable; the points marked with crosses are the combinations of these parameters for which the system was observed to be unstable. It is clear from Fig. 7 that the stability boundary predicted using the first-order Galerkin formulation is in close agreement with the stability observed experimentally. We were particularly interested in detecting the loss of stability as τ_1 increases (recall that $\tau(t) = \tau_1 + \tau_2 \sin(t)$ in Eq. (43)), which is reliably detected. The small difference between the predicted and observed stability boundaries may be attributed to error in model parameters and unmodeled effects. In Fig. 8, we show the time response of the system in two stable cases: $\tau(t) = 10 + 5\sin(t)$ ms and $\tau(t) = 10 + 6\sin(t)$ ms. The time response is shown for two unstable cases in Fig. 9: $\tau(t) = 11 + 5\sin(t)$ ms and $\tau(t) = 11 + 6\sin(t)$ ms.

We now use the proposed optimization-based framework to stabilize Eq. (41) where $\tau_1 = 11$ ms and $\tau_2 = 6$ ms. (The time response of the system for this combination of delay parameters is

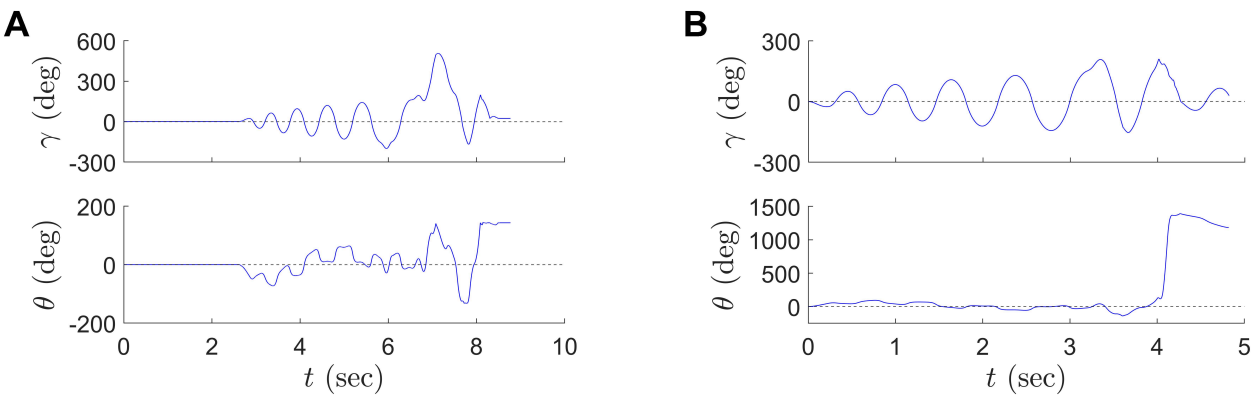

Figure 9: Unstable response of the inverted pendulum (γ) and rotary arm (θ) using feedback gains $\mathbf{K} = [-2, 30, -2, 2.5]^{\mathrm{T}}$ with a time-periodic delay: (A) $\tau(t) = 11 + 5\sin(t)$ ms and (B) $\tau(t) = 11 + 6\sin(t)$ ms.

shown in Fig. 9(B), when the original set of feedback gains $\mathbf{K}$ is used.) The minimization problem is solved using the Nelder–Mead algorithm in MATLAB® via the `fminsearch` function. The optimal feedback gains are $\mathbf{K}^* = [-2.1811, 30.4980, -1.4500, 2.8618]^{\mathrm{T}}$; the objective function value at this solution is $J^* = 3.6746 \times 10^{-11}$ and the spectral radius is 6.0619×10^{-6}. A second set of experiments is now performed, using optimal feedback gains $\mathbf{K}^*$. Recall that parameters $\tau_1 = 11$ ms and $\tau_2 = 6$ ms resulted in an unstable closed-loop system when the original feedback gains $\mathbf{K}$ were used (see Fig. 9(B)). Repeating this experiment using optimal feedback gains $\mathbf{K}^*$, we find that the system is now stable; the time response is shown in Fig. 10. Note that the oscillations in the angle of the pendulum (γ) and rotary arm (θ) are very small. In fact, the system remains stable for many parameter combinations that originally caused instability (indicated with crosses in Fig. 7). Increasing τ_1 while holding $\tau_2 = 6$ ms, we observe that the system remains stable up to $\tau_1 = 17$ ms (Fig. 11(A)). Although the pendulum remains upright ($\gamma \approx 180°$), notice that large oscillations appear in the response as the system recovers from the application of an external disturbance force at $t \approx 15$ s and $t \approx 27$ s. Increasing τ_1 further, we find that the system is unstable

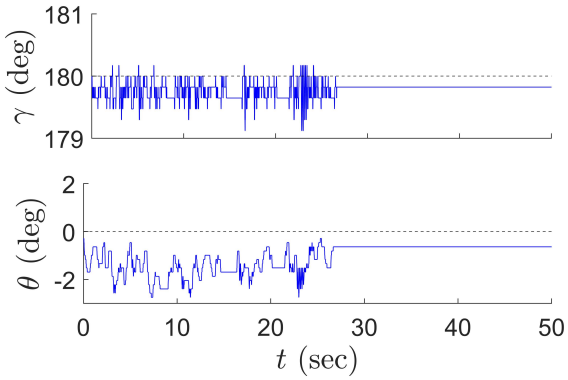

Figure 10: Stable response of the inverted pendulum (γ) and rotary arm (θ) using feedback gains $\mathbf{K}^* = [-2.1811, 30.4980, -1.4500, 2.8618]^{\mathrm{T}}$ with a time-periodic delay of $\tau(t) = 11+6\sin(t)$ ms.

when $\tau_1 = 18$ ms (Fig. 11(B)). Note, however, that these results were obtained using feedback gains $\mathbf{K}^*$ that were optimized for $\tau_1 = 11$ ms and $\tau_2 = 6$ ms; if larger delays are anticipated, the optimization procedure can be used to find a different set of feedback gains for the given delay parameters.

6 Conclusions

In this paper, we have first presented two approaches for applying the Galerkin approximation method to the analysis of second-order DDEs with time-periodic delays. As discussed and demonstrated, the second-order Galerkin formulation results in spurious Floquet multipliers, which limits its utility in pole-placement problems. Next, we have proposed an optimization-based framework for pole placement in time-delay systems, using the first-order Galerkin formulation (which does not introduce spurious Floquet multipliers). Finally, we validated the proposed approach experimentally using a rotary inverted pendulum apparatus with inherent sensing delays as well as additional time-periodic state-feedback delays that were introduced deliberately. This otherwise un-

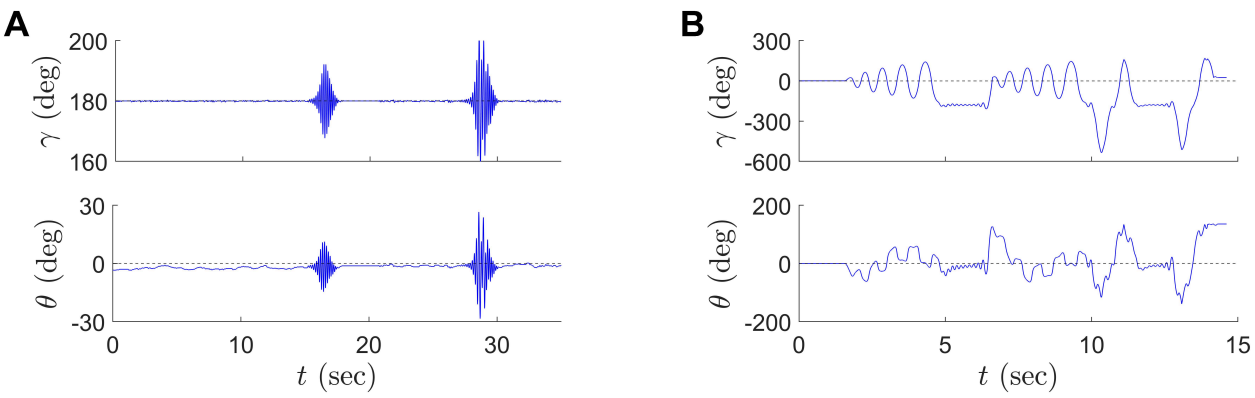

Figure 11: Response of the inverted pendulum (γ) and rotary arm (θ) using feedback gains $\mathbf{K}^* = [-2.1811, 30.4980, -1.4500, 2.8618]^{\mathrm{T}}$ with a time-periodic delay: (A) $\tau(t) = 17 + 6\sin(t)$ ms (stable) and (B) $\tau(t) = 18 + 6\sin(t)$ ms (unstable).

stable system was successfully stabilized using the proposed approach and the time-delay stability margin was increased.

The approach presented in this work can be extended to systems in which the coefficients are time-periodic, as might be encountered in studies on linear oscillators and rotor dynamics. It would be valuable to conduct further experimental validation since very limited literature exists on the validation of stabilization techniques for time-delay systems with time-periodic delays. It would also be useful to explore the effect of adding constraints to the optimization problem. An unconstrained optimization problem was solved in this work; however, practical systems are typically constrained by limits on the control effort, energy usage, and other factors.

Acknowledgments

The authors thank Dr. Ketan P. Detroja for providing the rotary inverted pendulum apparatus used in Sec. 5.

Funding Statement

C.P.V. gratefully acknowledges the Department of Science and Technology for funding this research through the Inspire fellowship (grant number DST/INSPIRE/04/2014/000972). The funders had no role in study design, data collection and analysis, decision to publish, or preparation of the manuscript.

References

[1] Yi, S., Nelson, P. W., and Ulsoy, A. G., 2010. *Time-Delay Systems: Analysis and Control Using the Lambert W Function*. World Scientific, Hackensack, NJ, USA. doi:10.1142/7759.

[2] Sadath, A., and Vyasarayani, C. P., 2015. "Galerkin approximations for stability of delay differential equations with distributed delays". *J Comput Nonlinear Dyn*, **10**(6), p. 061024. doi:10.1115/1.4030153.

[3] Asl, F. M., and Ulsoy, A. G., 2003. "Analysis of a system of linear delay differential equations". *J Dyn Syst Meas Control*, **125**(2), pp. 215–223. doi:10.1115/1.1568121.

[4] Jarlebring, E., and Damm, T., 2007. "The Lambert W function and the spectrum of some multidimensional time-delay systems". *Automatica*, **43**(12), pp. 2124–2128. doi:10.1016/j.automatica.2007.04.001.

[5] Yi, S., Nelson, P. W., and Ulsoy, A. G., 2007. "Survey on analysis of time delayed systems via the Lambert W function". *Dyn Contin Discrete Impulsive Syst*, **14**(S2), pp. 296–301.

[6] Wahi, P., and Chatterjee, A., 2005. "Asymptotics for the characteristic roots of delayed dynamic systems". *J Appl Mech*, **72**(4), pp. 475–483. doi:10.1115/1.1875492.

[7] Vyasarayani, C. P., 2012. “Galerkin approximations for higher order delay differential equations”. *J Comput Nonlinear Dyn,* **7**(3), p. 031004. doi:10.1115/1.4005931.

[8] Kalmár-Nagy, T., 2009. “Stability analysis of delay-differential equations by the method of steps and inverse Laplace transform”. *Differ Equ Dyn Syst,* **17**(1–2), pp. 185–200. doi:10.1007/s12591-009-0014-x.

[9] Insperger, T., and Stépán, G., 2011. *Semi-Discretization for Time-Delay Systems: Stability and Engineering Applications*. Springer, New York, NY, USA. doi:10.1007/978-1-4614-0335-7.

[10] Wahi, P., and Chatterjee, A., 2005. “Galerkin projections for delay differential equations”. *J Dyn Syst Meas Control*, **127**(1), pp. 80–87. doi:10.1115/1.1870042.

[11] Butcher, E. A., Ma, H., Bueler, E., Averina, V., and Szabo, Z., 2004. “Stability of linear time-periodic delay-differential equations via Chebyshev polynomials”. *Int J Numer Methods Eng,* **59**(7), pp. 895–922. doi:10.1002/nme.894.

[12] Breda, D., Maset, S., and Vermiglio, R., 2005. “Pseudospectral differencing methods for characteristic roots of delay differential equations”. *SIAM J Sci Comput,* **27**(2), pp. 482–495. doi:10.1137/030601600.

[13] Wu, Z., and Michiels, W., 2012. “Reliably computing all characteristic roots of delay differential equations in a given right half plane using a spectral method”. *J Comput Appl Math,* **236**(9), pp. 2499–2514. doi:10.1016/j.cam.2011.12.009.

[14] Pekař, L., and Gao, Q., 2018. “Spectrum analysis of LTI continuous-time systems with constant delays: a literature overview of some recent results”. *IEEE Access,* **6**, pp. 35457–35491. doi:10.1109/ACCESS.2018.2851453.

[15] Sadath, A., and Vyasarayani, C. P., 2015. "Galerkin approximations for stability of delay differential equations with time periodic delays". *J Comput Nonlinear Dyn,* **10**(6), p. 061008. doi:10.1115/1.4028631.

[16] Ahsan, Z., Sadath, A., Uchida, T. K., and Vyasarayani, C. P., 2015. "Galerkin–Arnoldi algorithm for stability analysis of time-periodic delay differential equations". *Nonlinear Dyn,* **82**(4), pp. 1893–1904. doi:10.1007/s11071-015-2285-9.

[17] Altintas, Y., and Chan, P. K., 1992. "In-process detection and suppression of chatter in milling". *Int J Mach Tools Manuf,* **32**(3), pp. 329–347. doi:10.1016/0890-6955(92)90006-3.

[18] Radulescu, R., Kapoor, S. G., and DeVor, R. E., 1997. "An investigation of variable spindle speed face milling for tool-work structures with complex dynamics, part 1: simulation results". *J Manuf Sci Eng,* **119**(3), pp. 266–272. doi:10.1115/1.2831103.

[19] Long, X., Insperger, T., and Balachandran, B., 2009. "Systems with periodic coefficients and periodically varying delays: semidiscretization-based stability analysis". In *Delay Differential Equations: Recent Advances and New Directions*, D. E. Gilsinn, T. Kalmár-Nagy, and B. Balachandran, eds. Springer, Boston, MA, USA, pp. 131–153. doi:10.1007/978-0-387-85595-0_5.

[20] Long, X., and Balachandran, B., 2010. "Stability of up-milling and down-milling operations with variable spindle speed". *J Vib Control,* **16**(7–8), pp. 1151–1168. doi:10.1177/1077546309341131.

[21] Sastry, S., Kapoor, S. G., DeVor, R. E., and Dullerud, G. E., 2001. "Chatter stability analysis of the variable speed face-milling process". *J Manuf Sci Eng,* **123**(4), pp. 753–756. doi:10.1115/1.1373649.

[22] Yilmaz, A., Emad, A.-R., and Ni, J., 2002. "Machine tool chatter suppression by multi-level random spindle speed variation". *J Manuf Sci Eng,* **124**(2), pp. 208–216. doi:10.1115/1.1378794.

[23] Liu, Z., and Liao, L., 2004. "Existence and global exponential stability of periodic solution of cellular neural networks with time-varying delays". *J Math Anal Appl,* **290**(1), pp. 247–262. doi:10.1016/j.jmaa.2003.09.052.

[24] Jiang, M., Shen, Y., and Liao, X., 2006. "Global stability of periodic solution for bidirectional associative memory neural networks with varying-time delay". *Appl Math Comput,* **182**(1), pp. 509–520. doi:10.1016/j.amc.2006.04.012.

[25] Engelborghs, K., Luzyanina, T., and Roose, D., 2002. "Numerical bifurcation analysis of delay differential equations using DDE-BIFTOOL". *ACM Trans Math Softw,* **28**(1), pp. 1–21. doi:10.1145/513001.513002.

[26] Butcher, E., and Mann, B., 2009. "Stability analysis and control of linear periodic delayed systems using Chebyshev and temporal finite element methods". In *Delay Differential Equations: Recent Advances and New Directions,* D. E. Gilsinn, T. Kalmár-Nagy, and B. Balachandran, eds. Springer, Boston, MA, USA, pp. 93–129. doi:10.1007/978-0-387-85595-0_4.

[27] Zhang, J., and Sun, J.-Q., 2009. "Robustness analysis of optimally designed feedback control of linear periodic systems with time-delay". In Proceedings of the ASME 2007 International Design Engineering Technical Conferences and Computers and Information in Engineering Conference, Las Vegas, NV, September 4–7, pp. 703–710. doi:10.1115/DETC2007-34438.

[28] Butcher, E. A., Bobrenkov, O., Nazari, M., and Torkamani, S., 2013. "Estimation and control in time-delayed dynamical systems using the Chebyshev spectral continuous time approxima-

tion and reduced Liapunov-Floquet transformation". In *Advances in Analysis and Control of Time-Delayed Dynamical Systems*, J.-Q. Sun and Q. Ding, eds. World Scientific, Singapore, pp. 219–264. doi:10.1142/9789814525503_0008.

[29] Nazari, M., Butcher, E. A., and Bobrenkov, O. A., 2014. "Optimal feedback control strategies for periodic delayed systems". *Int J Dyn Control,* **2**(1), pp. 102–118. doi:10.1007/s40435-013-0053-6.

[30] Ma, H., Deshmukh, V., Butcher, E., and Averina, V., 2003. "Controller design for linear time-periodic delay systems via a symbolic approach". In Proceedings of the 2003 American Control Conference, Denver, CO, June 4–6, pp. 2126–2131. doi:10.1109/ACC.2003.1243388.

[31] Ma, H., Deshmukh, V., Butcher, E., and Averina, V., 2005. "Delayed state feedback and chaos control for time-periodic systems via a symbolic approach". *Commun Nonlinear Sci Numer Simul,* **10**(5), pp. 479–497. doi:10.1016/j.cnsns.2003.12.007.

[32] Borgioli, F., Hajdu, D., Insperger, T., Stepan, G., and Michiels, W., 2020. "Pseudospectral method for assessing stability robustness for linear time-periodic delayed dynamical systems". *Int J Numer Methods Eng*, **121**(16), pp. 3505–3528. doi:10.1002/nme.6368.

[33] Sadath, A., and Vyasarayani, C. P., 2015. "Galerkin approximations for stability of delay differential equations with time periodic coefficients". *J Comput Nonlinear Dyn*, **10**(2), p. 021011. doi:10.1115/1.4026989.

[34] Kandala, S. S., 2020. "Pole placement and reduced-order modelling of time-delayed systems using galerkin approximations". PhD thesis, Indian Institute of Technology Hyderabad, Telangana, India.

[35] Vyasarayani, C. P., Subhash, S., and Kalmár-Nagy, T., 2014. "Spectral approximations for characteristic roots of delay differential equations". *Int J Dyn Control,* **2**(2), pp. 126–132. doi:10.1007/s40435-014-0060-2.

[36] Gottlieb, D., and Orszag, S. A., 1977. *Numerical Analysis of Spectral Methods: Theory and Applications*. Society for Industrial and Applied Mathematics, Philadelphia, PA, USA. doi:10.1137/1.9781611970425.

[37] Kovacic, I., Rand, R., and Sah, S. M., 2018. "Mathieu's equation and its generalizations: overview of stability charts and their features". *Appl Mech Rev,* **70**(2), p. 020802. doi:10.1115/1.4039144.

[38] Apkarian, J., Lévis, M., and Martin, P., 2016. *Instructor Workbook: QUBE-Servo 2 Experiment for MATLAB/Simulink Users*. Quanser Inc., Markham, ON, Canada.

[39] Apkarian, J., Karam, P., and Lévis, M., 2012. *Student Workbook: Inverted Pendulum Experiment for LabVIEW Users*. Quanser Inc., Markham, ON, Canada.